

# Counting unstable periodic orbits in noisy chaotic systems: A scaling relation connecting experiment with theory

Xing Pei, Kevin Dolan, and Frank Moss<sup>a)</sup>

*Center for Neurodynamics, University of Missouri at St. Louis, St. Louis, Missouri 63121*

Ying-Cheng Lai

*Departments of Physics and Astronomy and of Mathematics, The University of Kansas, Lawrence, Kansas 66045*

(Received 4 May 1998; accepted for publication 17 August 1998)

The experimental detection of unstable periodic orbits in dynamical systems, especially those which yield short, noisy or nonstationary data sets, is a current topic of interest in many research areas. Unfortunately, for such data sets, only a few of the lowest order periods can be detected with quantifiable statistical accuracy. The primary observable is the number of encounters the general trajectory has with a particular orbit. Here we show that, in the limit of large period, this quantity scales exponentially with the period, and that this scaling is robust to dynamical noise. © 1998 American Institute of Physics. [S1054-1500(98)00904-5]

**The recent development of new methods for detecting and counting unstable periodic orbits (UPOs) in short, noisy time series have opened the door to studies of chaos in systems of unknown dynamics that were previously inaccessible. Unfortunately, when applied to data sets of typical experimental lengths, these methods are unable to detect orbits with periods greater than about four. But can it be maintained that chaos has been demonstrated in such experimental systems, given that the structure of the strange attractor is built upon an infinite set of UPOs? Can these three or four orbits be convincingly connected to the infinite set? Here we investigate the possibility of a scaling relation to make this connection. We derive approximate expressions for the scaling exponents in two ways, beginning with a well known scaling relation. Our numerical results test the accuracy of the scaling for noise contaminated dynamics of both discrete and continuous systems. We find exponential scaling which is robust to dynamical noise, and an example from experimental sensory biology is given.**

## I. INTRODUCTION

The detection of chaotic attractors from time series generated by experimental systems of unknown dynamics is a problem of continuing interest in a variety of fields. Techniques based on ensemble averages of the metric properties of attractors,<sup>1,2</sup> for example, measurements of one or more of the Lyapunov exponents<sup>3-5</sup> or fractal dimensions,<sup>6-11</sup> have been enormously successful. However, their requirements for long, relatively noise free data sets have limited their applications. Various predictor and other methods<sup>12,13</sup> have suffered similar limitations, though recent progress with nonlinear predictors<sup>14,15</sup> has been reported.

Recently, however, new methods based on the detection

of unstable periodic orbits (UPOs) of low period have been developed. Two of these, which exploit the topological properties of attractors, have been particularly successful, though in very different applications. The first, called the method of close returns (CR),<sup>16,17</sup> is suitable for finding UPOs with periods up to at least  $p=30$  in long data sets (typically  $10^7$  or  $10^8$ ) from relatively noise free, stationary numerical or physical data.<sup>17-19</sup> The second, called the topological recurrence (TR) method,<sup>20</sup> is statistically based and useful for short (a few  $\times 10^2$  to  $10^3$ ), noisy data sets, such as those typical of nonstationary biological systems.<sup>21-23</sup> In contrast to some metric and other methods, the TR method is able to distinguish between UPOs and stable periodic orbits (SPOs). This advantage arises because it specifically searches for the topological signature of instability, that is, intersections of unstable and stable manifolds, in the returns. This property has been crucial in recent experiments in sensory biology, wherein control parameter induced bifurcations between UPOs and SPOs have been discovered in diverse sensory neurons.<sup>21,23</sup> A third method, based on a dynamical transformation (DT)<sup>24</sup> of the near neighborhoods of periodic orbits in phase space, has also been successfully used to detect UPOs in data sets from noise contaminated systems.<sup>24,25</sup> The TR and DT methods have recently been reviewed and compared.<sup>26</sup>

Two facts, relevant to these recent methods, motivate this work: (1) the primary experimental observable is the number of times a UPO of period  $p$  is encountered in a time series; and (2) (obviously) the largest detectable period is finite. In the case of the TR and DT methods, this period is not larger than four.<sup>26</sup> But the structure of chaotic attractors is a countable infinity of UPOs.<sup>27-33</sup> While the detection of as many as 30 orbits may be convincing, as with the CR or other methods which find the shadows of reference orbits, the measurement of only three or four, as with DT and TR, can hardly be put forth as evidence of the infinite set. Unfortunately, the CR method is not useful for short, noisy, for example, biological, systems. In contrast, the DT and TR

<sup>a)</sup>Electronic mail: mossf@umslvma.umsl.edu

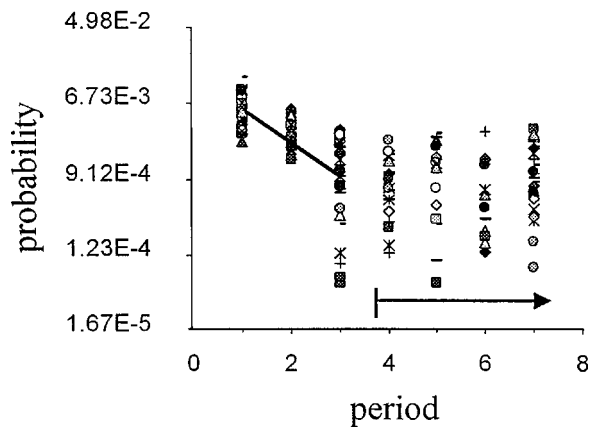


FIG. 1. The probability to observe unstable periodic orbits of period  $p$  in the sensory mechanoreceptive system of the crayfish, *Procambarus clarkii*. Neural recordings were made from the caudal photoreceptor cell, a pace-maker (oscillator) embedded within and synaptically connected to the 6th ganglion, a small network of interneurons that processes noisy hydrodynamic signals from the hair receptors arrayed on the animal's tailfan. The hair receptors were periodically stimulated by a sinusoidal water motion applied to the tailfan. These data represent 44 files (different symbols), chosen from more than 1000 on the basis of large responses at  $p=2$ . The data were obtained for a variety of different experimental conditions from 19 different animals, and thus represent the general behavior to be expected for such systems. The vertical axis is the natural logarithm of the probability, obtained by counting the number of encounters with UPOs in a data file and subtracting the number found in a suitable surrogate. See Refs. 20–23 for details. The solid line represents an exponential scaling of the probability with period  $p$  with slope  $-0.51$ . The arrow marks the region of behavior indistinguishable from the surrogates.

methods have successfully detected UPOs in data sets wherein they were invisible to other methods. However, because they exploit much more specific or restrictive (than simply close returns) signatures of encounters with UPOs, they sacrifice the ability to find orbits of larger period.

Observations of a typical biological system with TR seem to indicate that the probability to observe UPOs decreases exponentially with increasing period,  $p$ . See, for example, Fig. 1. This suggests that a scaling relation might exist by means of which the few experimentally detectable orbits can be connected to the infinite set. The analogy with universal scalings near thermodynamic phase transitions is evident and has been previously advanced,<sup>32–37</sup> and orbital return times in two, nonhyperbolic, chaotic systems have been studied.<sup>38,39</sup> The purpose of this work is to derive from this a simple and physically motivated, though approximate, theory of the probability  $\Phi(p)$ , that an orbit of period  $p$  is encountered in a time series of finite length. One way to do this is to begin with the well known probability of finding a shadow, that is, a trajectory of length  $n$ , within a distance  $\epsilon$  of a reference orbit, which is approximately  $\langle P(n, \epsilon) \rangle \approx \epsilon^{\alpha(\mathbf{x})} \exp(-nK_1)$ , where  $K_1$  is the metric entropy, and  $\alpha(\mathbf{x})$  is a dimension which depends on the trajectory  $\mathbf{x}$ , that is on an initial condition. We lump all orbits of the same period together by estimating the cumulative encounter probability. This is exactly what the TR and DT methods detect. We find that, in the limit of large  $p$ , the encounter probability,  $\Phi(p)$ , indeed scales exponentially with an exponent,  $Q$ , which is

related to the metric and topological entropies and to the largest Lyapunov exponent of the attractor:

$$\Phi(p) \sim \epsilon^{\text{const}} \exp[-Qp]. \quad (1)$$

We test the exponential behavior, where  $Q$  is a constant related to  $K_0$ ,  $K_1$ , and  $\lambda$ , for periods up to  $p=30$  with numerical experiments using a somewhat modified version of the CR method on long, noise free data sets of the logistic and Hénon maps, and on the Lorenz dynamical system. In addition, our numerical experiments confirm the prefactor  $\epsilon^{\text{const}}$ .<sup>40</sup> Moreover, because the Hénon map is one of the few model systems for which, in principle, an arbitrarily large number of orbits can be analytically computed by a numerical algorithm,<sup>41,42</sup> we can thus provide a test independent of the CR or TR algorithms.

A primary objective is to test the robustness of the scaling relation on systems contaminated with noise. The motivation for this is provided by sensory biology, where data sets of limited length from noisy dynamics are ubiquitous. We mention that our theory applies strictly only to hyperbolic systems, whereas nonhyperbolic motion is generic to real physical systems.<sup>38,39</sup> However, as we show here, the scaling appears to be valid even for nonhyperbolic systems, of which the Hénon and Lorenz systems are examples. Finally, we mention that because there is an infinity of stable periodic orbits (SPOs) embedded in the attractors of nonhyperbolic systems, search algorithms which can distinguish between UPOs and SPOs, such as the TR algorithm, have an inherent advantage for analyses of real physical systems. A preliminary account of this work is to be given elsewhere.<sup>43</sup>

This paper is organized in the following way. In Sec. II we outline the approximate theory, which we develop from two different approaches. In Sec. III we discuss our modifications of the CR algorithm. We use it to test the scaling relation for the logistic and Hénon maps, including tests of its robustness in the presence of additive noise. In addition, we apply the analysis to the Lorenz system. Finally, in Sec. IV, we summarize our results and comment on their applicability to searches for UPOs in biological systems.

## II. THEORY

To gain intuition for the validity of the scaling relation, we first consider a simple class of one-dimensional chaotic systems defined on the unit interval: the tent map  $[x_{(n+1)} = 2x_n$  if  $x_n < 1/2$ , and  $x_{(n+1)} = 2(1-x_n)$  if  $x_n \geq 1/2]$ , or the doubling transformation  $[x_{(n+1)} = 2x_n \bmod(1)]$ . It is known that both maps generate a chaotic attractor, and the invariant density generated by a trajectory originated from a random initial condition (a typical trajectory) is uniform in the unit interval.<sup>44</sup> Thus in order for a trajectory to stay in a small  $\epsilon$ -neighborhood of a periodic orbit of period  $p$ , the trajectory must fall within  $\epsilon e^{-\lambda p}$  of any one of the components of the periodic orbit, where  $\lambda = \ln 2$  is the Lyapunov exponent of the chaotic attractor. Since the invariant density is uniform, the probability for a typical trajectory to fall in an interval is equal to the length of this interval. Note that there are  $2^p$  orbits of period  $p$  in the tent map. We have  $\Phi(p) = \sum_{i=1}^{2^p} \mu_i(p) \epsilon e^{-\lambda p}$ , where  $\mu_i(p) = 2^{-p}$  is the weight, or

natural measure, associated with the  $i$ th orbit of period  $p$  in the tent map. This consideration also applies to chaotic systems with smooth invariant densities such as the one-dimensional logistic map  $x_{(n+1)} = ax_n(1 - x_n)$  at  $a = 4$ . In such a case, we have, for the probability,  $\Phi_{\text{traj}}(\epsilon, p)$ , for a trajectory to fall within a small interval of length  $\epsilon e^{-\lambda p}$  centered at a periodic point  $x_p$ , the following,

$$\Phi_{\text{traj}}(\epsilon, p) = \int_{x_p - \epsilon \exp(-\lambda p)/2}^{x_p + \epsilon \exp(-\lambda p)/2} \rho(x) dx \approx \epsilon \exp(-\lambda p), \quad (2)$$

where  $\rho(x)$  is the smooth invariant density of the chaotic attractor. Summing all periodic orbits of period  $p$  and using  $\mu_i(p) \sim \exp(-\lambda p)$ , we have  $\Phi(p) \sim N(p) \exp(-2\lambda p)$ , where  $N(p) \sim \exp(K_0 p)$ , and  $K_0$  is the topological entropy of the chaotic attractor.

Chaotic systems with smooth invariant densities are rare. Often, the density function contains an infinite number of singularities.<sup>44</sup> Thus it is not apparent whether the scaling relation holds in general. Nonetheless, heuristic arguments can be made to lend credence to the validity of an exponential scaling of the encounter probability. In the sequel, we present two different approaches to the approximate derivation of Eq. (1), both yielding the same exponential scaling relation, but with slightly different constants,  $Q$ .

### A. Derivation based on a property of the metric entropy

In this approach we make use of the well known, but not rigorously derived, property that the length of a shadow orbit scales exponentially with the metric entropy. We restrict our consideration to systems with chaotic attractors. To find the encounter probability with a periodic orbit of period  $p$ , we utilize the concept of the generalized entropies  $K_q$ .<sup>45</sup> Given a chaotic system, described either by a smooth autonomous flow or by a discrete map, the generalized entropies  $K_q$  can be defined by considering the probability for a typical trajectory to fall within a small  $\epsilon$ -neighborhood of a target orbit of length  $t$  embedded in the chaotic attractor. This target orbit can be either periodic or chaotic. Let  $\mathbf{x}$  be the starting point of the target orbit (in the case of a periodic orbit,  $\mathbf{x}$  can be any point of the orbit) and let  $P(\epsilon, t; \mathbf{x})$  denote the probability. For chaotic systems, it is assumed<sup>35</sup> that  $P(\epsilon, t; \mathbf{x})$  scales with  $\epsilon$  and  $t$  as,

$$P(\epsilon, t; \mathbf{x}) \approx \epsilon^{\alpha(\mathbf{x})} \epsilon^{-\kappa(\mathbf{x}, t)t}, \quad (3)$$

in the limit  $\epsilon \rightarrow 0$  and  $t \rightarrow \infty$ , where  $\alpha(\mathbf{x})$  is the pointwise dimension of the point  $\mathbf{x}$  and  $\kappa(\mathbf{x}, t)$  is the local entropy of the target orbit. The information dimension  $D_1$  and the metric entropy  $K_1$  of the chaotic attractor can be defined as

$$\langle P(\epsilon, t; \mathbf{x}) \rangle \approx \epsilon^{D_1} \epsilon^{-K_1 t}, \quad \text{for } \epsilon \rightarrow 0 \text{ and } t \rightarrow \infty, \quad (4)$$

where  $\langle \rangle$  denotes the ensemble average over many typical trajectories on the chaotic attractor. Now consider the case where the target orbit is a periodic orbit of period  $p$ . There are  $N(p) \propto (1/p) \exp(K_0 p)$  such orbits, where  $K_0$  is the topological entropy. Denote the orbit by  $\mathbf{x}_{ip}$  where  $i = 1, \dots, N(p)$  (here for simplicity of notation we just use  $\mathbf{x}_{ip}$ , to denote the orbit which actually has  $p$  components). The probability for a

typical trajectory to come close to this orbit is then given by Eq. (3) where  $\mathbf{x}$  is replaced by  $\mathbf{x}_{ip}$ , and the time  $t$  is replaced by the period  $p$ . The encounter probability  $\Phi(p)$  with a periodic orbit of period  $p$  is then the cumulative probability of encounters with all  $N(p)$  periodic orbits. We have

$$\Phi(p) = \sum_{i=1}^{N(p)} \mu_i(p) P(\epsilon, p; \mathbf{x}_{ip}), \quad (5)$$

where the weight  $\mu_i(p)$  is the natural measure<sup>46</sup> associated with the periodic orbit  $\mathbf{x}_{ip}$ . This natural measure can be expressed in terms of the largest expanding eigenvalue  $L_1(\mathbf{x}_{ip})$  of the periodic orbit<sup>47-49</sup> as

$$\mu_i = 1/L_1(\mathbf{x}_{ip}) \equiv \exp[-\lambda_i(p)p], \quad (6)$$

where  $\lambda_i(p) > 0$  is the unstable Lyapunov exponent of the periodic orbit, and the exponent varies among all the period- $p$  orbits. For  $p$  large, we expect  $\lambda_i(p)$  to be close to  $\lambda$ , the Lyapunov exponent of the entire chaotic attractor. We write  $\lambda_i(p) = \lambda + \Delta\lambda_i(p)$ . This consideration also applies to the local dimension and entropy. Using Eq. (4) we can write  $\alpha(\mathbf{x}_{ip}) = D_1 + \Delta\alpha(\mathbf{x}_{ip})$  and  $\kappa(\mathbf{x}_{ip}, p) = K_1 + \Delta\kappa(\mathbf{x}_{ip}, p)$ . Substituting these two expressions, Eqs. (3) and (6), into Eq. (5), we obtain

$$\Phi(p) \propto e^{-\lambda p} e^{-\kappa_1 p} e^{D_1} \sum_{i=1}^{N(p)} e^{-[\Delta\lambda_i(p) + \Delta\kappa(\mathbf{x}_{ip}, p)]p} \epsilon^{\Delta\alpha(\mathbf{x}_{ip})}. \quad (7)$$

Since  $N(p)$  grows exponentially as  $p$  increases, we expect  $N(p)$  to be a large number when  $p$  is large. Thus roughly  $\Delta\lambda_i(p)$ ,  $\Delta\kappa(\mathbf{x}_{ip}, p)$  and  $\Delta\alpha(\mathbf{x}_{ip})$  can be treated as random variables of zero mean. By the law of large numbers, the summation in (7) can be regarded as a random variable centered at one with a Gaussian probability distribution. The width of the distribution behaves like  $1/\sqrt{N(p)}$   $\propto \exp(-K_0 p/2) \rightarrow 0$  as  $p \rightarrow \infty$ . Thus (7) becomes

$$\Phi(p) \propto e^{-(\lambda + K_1 - K_0)p}. \quad (8)$$

In typical chaotic systems the quantities  $\lambda$ ,  $K_1$  and  $K_0$  have similar numerical values, but since  $K_0 \geq K_1$ , the exponent  $Q$  in Eq. (1) can be expected to underestimate  $\lambda$ .<sup>50</sup>

### B. Derivation based on natural measure of periodic orbits

Although the above derivation of the scaling relation is quite general, its starting point, Eq. (3), is only an assumption. Here we wish to point out that for chaotic systems described by two-dimensional hyperbolic maps  $\mathbf{M}(\mathbf{x})$ ,<sup>51</sup> a derivation can be made starting from the first principles.<sup>47</sup> A hyperbolic periodic orbit has a distinct set of expanding (unstable) and contracting (stable) directions. Consider the encounter probability with one of the periodic orbits of period  $p$ . The periodic orbit is thus a fixed point of the  $p$ -times iterated map  $\mathbf{M}^{(p)}(\mathbf{x})$ . Denote the fixed point by  $\mathbf{x}_{ip}$ , and there are  $N(p) \propto \exp(K_0 p)$  such fixed points. Following Grebogi, Ott and Yorke,<sup>47</sup> we cover the chaotic attractor with a grid of partitioning boxes, each being confined by segments of the stable and unstable manifolds. Typically,  $\mathbf{x}_{ip}$  is contained in a box  $C_i$ . Since the boxes are constructed by using the stable and unstable foliations of the chaotic attractor,

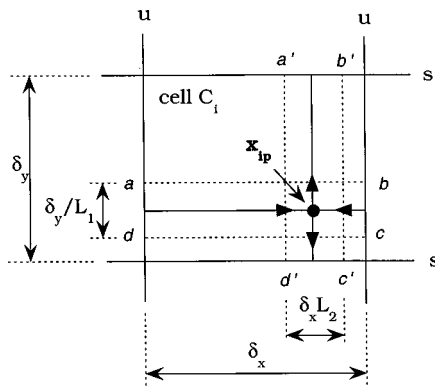


FIG. 2. Schematic illustration of a partitioning box containing a periodic orbit of period  $p$  and the fraction of initial conditions that stay close to this orbit in  $p$  iterations.

they can be made arbitrarily small. Thus each box can be regarded as being rectangular, as shown schematically in Fig. 2, where the horizontal and vertical sides are segments of the stable and unstable manifolds, respectively. Assume there is a segment of  $p$  points on a typical trajectory, denoted by  $\{\mathbf{x}(0), \mathbf{x}(1), \dots, \mathbf{x}(p)\}$  which stays close to  $\mathbf{x}_{ip}$ . One way for this to occur is for both the beginning point  $\mathbf{x}(0)$  and the ending point  $\mathbf{x}(p)$  of the segment to be contained in the small box  $C_i$ . In order to estimate the probability for such an encounter, imagine we choose a large number of initial conditions on the chaotic attractor according to the natural measure. The probability of encounter with  $\mathbf{x}_{ip}$  is then approximately the fraction of initial conditions starting in  $C_i$  but still being in  $C_i$  in  $p$  iterations. Let  $\delta_x$  and  $\delta_y$  be the lengths of the horizontal and the vertical sides of  $C_i$ , respectively. Since the dynamics is contracting in the horizontal direction and expanding in the vertical direction, we see that the rectangle  $abcd$  maps to another rectangle  $a'b'c'd'$  in  $p$  iterations. The sizes of the rectangles  $abcd$  and  $a'b'c'd'$  are  $\delta_x \cdot [\delta_y/L_1(\mathbf{x}_{ip})]$  and  $[\delta_x/L_2(\mathbf{x}_{ip})] \cdot \delta_y$ , respectively, where  $L_1(\mathbf{x}_{ip}) > 1$  and  $L_2(\mathbf{x}_{ip}) < 1$  are the unstable (expanding) and stable (contracting) eigenvalues of the fixed point  $\mathbf{x}_{ip}$ . Initial conditions chosen from  $C_i$  but not in the rectangle  $abcd$  map out of  $C_i$  in  $p$  iterations. Since the natural measure is uniform in the unstable directions for a chaotic attractor, the fraction of initial conditions starting in  $C_i$  but remaining in  $C_i$  after  $p$  iterations is given by  $|ad|/|a'd'| = [\delta_y/L_1(\mathbf{x}_{ip})]/\delta_y = 1/L_1(\mathbf{x}_{ip}) \equiv \exp[-\lambda_i(p)p]$ , where  $\lambda_i(p) > 0$  is the unstable Lyapunov exponent of the  $i$ th unstable periodic orbit of period  $p$ . Thus the encounter probability with this periodic orbit is  $\exp[-\lambda_i(p)p]$ .

Since there are  $N(p)$  periodic orbits of period  $p$ , the cumulative encounter probability with a period- $p$  orbit is

$$\Phi(p) = \sum_{i=1}^{N(p)} \mu_i(p) \exp[-\lambda_i(p)p], \quad (9)$$

where  $\mu_i(p) = \exp[-\lambda_i(p)p]$  is the natural measure associated with the  $i$ th orbit of period  $p$ . For  $p$  large we can write  $\lambda_i(p) = \lambda + \Delta\lambda_i(p)$ . Since  $N(p)$  grows exponentially as  $p$  increases, we expect  $N(p)$  to be a large number when  $p$  is high. Thus we obtain

$$\Phi(p) \approx \exp(-2\lambda p) \sum_{i=1}^{N(p)} \exp[2\Delta\lambda_i(p)p]. \quad (10)$$

Following the same argument from Eq. (7) to Eq. (8), we have

$$\Phi(p) \approx \exp(-2\lambda p) N(p) \approx \exp(-2\lambda + K_0)p. \quad (11)$$

Thus we again predict exponential scaling of the encounter probability with well characterized measures associated with the attractor, and again the constant  $Q$  in Eq. (1) underestimates  $\lambda$ .

Strictly speaking, the argument above is valid only for hyperbolic systems for which a good partition of the phase space can be made so that the shorter line segments  $a'b'$  and  $ad$  in Fig. 2 are completely contained in the box  $C_i$ . Such a partition is called the Markov partition.<sup>52</sup> Most chaotic systems arising in physical situations are, however, nonhyperbolic. For nonhyperbolic systems it may happen that a grid of boxes in which each box  $C_i$  looks like the box in Fig. 2 cannot be constructed because of the set of an infinite number of tangency points between the stable and unstable manifolds.<sup>44</sup> Nevertheless, the fact that exponential scaling can be obtained via two different arguments leads us to believe that it is valid for chaotic systems arising in more realistic situations.

### III. NUMERICAL TESTS

The CR algorithm is a search technique that assumes the existence of a set of periodic orbits in a time series. We look for points near enough to the orbits that they evolve for a time in its  $\epsilon$ -neighborhood. Such close return segments can be located in the original time series  $x(i)$  ( $i=1,2,\dots,N$ ), where  $N$  is the total number of datum points in the set, without embedding. The close returns can be found by plotting a histogram of the 1's given by the following quantity,<sup>17</sup>

$$|x(i) - x(i+n)| \begin{cases} < \epsilon \rightarrow 1 \\ > \epsilon \rightarrow 0 \end{cases}. \quad (12)$$

Such a histogram shows peaks at values of  $n$  corresponding to the periods  $p$ . The amplitudes of these peaks are the experimental values of the encounter probability  $\Phi(p)$ . We have modified this algorithm in the following way. In the original CR algorithm, individual close returns were tabulated and contributed to the histogram as specified by Eq. (12). In our modification, when a close return is found at any index  $n$ , then we additionally require  $n$  sequential close returns to the neighborhood  $\epsilon$  in order for a 1 to be written to the histogram. Thus only shadow trajectories of length  $n$  contribute to the histogram. Examples of the maxima of the histograms are shown by the figures in the following sections.

We now give numerical evidence for exponential scaling using data generated by the logistic and Hénon maps and the Lorenz system. We use the modified CR algorithm discussed above. As a check, we additionally test the Hénon map with the method of Refs. 41 and 42. We generate files of total length  $N$  the order of  $10^8$ , and search with neighborhood size  $\epsilon$  in the range  $10^{-4}$ – $10^{-1}$  for the parameter values given.

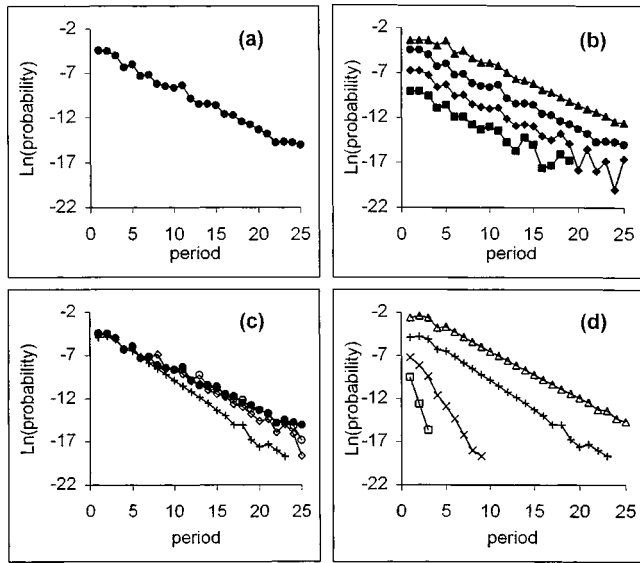


FIG. 3. Scaling of the encounter probability versus period  $p$ , of UPOs in the logistic map for  $a=3.9300$ . (a) The scaling for  $\xi=0$  and  $\epsilon=0.01$ . (b) A study of the effect of the neighborhood size with zero noise, for  $\epsilon=0.1$  (triangles),  $0.01$  (circles),  $0.001$  (diamonds), and  $0.0001$  (squares). (c) The scaling for various noise intensities  $\xi=0$  (solid circles),  $0.0001$  (open circles),  $0.0001$  (open diamonds), and  $0.01\epsilon$  (crosses). (d) A study of the effect of  $\epsilon$  with noise  $\xi=0.01$ , for  $\epsilon=0.1$  (triangles),  $0.01\epsilon$  (plus signs),  $0.001$  (crosses), and  $0.0001$  (squares). In the iteration of the map,  $10^4$  points were allowed for transients to die, and the total number of points varied from  $1 \times 10^8$  to  $5 \times 10^8$ . Numerical agreement with Eq. (1) is excellent for values of  $\xi \ll \epsilon$  as expected. Note also that the results shown in (b) are in excellent agreement with the behavior predicted by the prefactor  $\epsilon^{(a)}$  in Eq. (1). The largest Lyapunov exponent,  $0.602$ , is underestimated by the slope of the numerical data in (a), for which  $Q=0.460 \pm 0.035$  (SE).

We compare the results for the noise free dynamics to those for noise intensities  $\xi$  in the range  $10^{-4} - 10^{-1}$ .

### A. The logistic map

The logistic map is given by

$$x_{n+1} = \alpha x_n (1 - x_n) + \xi_n, \quad (13)$$

where  $\xi_n$  is the noise. We have chosen the bifurcation parameter  $a=3.9300$ . For  $\xi_n=0$ , the results are shown in Fig. 3(a). A least-squares fit of  $\Phi(p) \sim \exp[-Qp]$  to the triangles gives  $Q=0.460 \pm 0.035$  (SE) which can be compared with the value  $\lambda=0.602$ , which we measured using a standard technique.<sup>53</sup> Note that the scaling is accurate (that is, the numerical results are well represented by a straight line on the semilog plot of Fig. 3) over more than two orders and for periods up to  $p=25$ . This procedure has been repeated for three noise intensities, taken from a uniform distribution  $[-\xi, \xi]$ , with  $\xi$  smaller than and equal to  $\epsilon$ . The results for various values of  $\epsilon$  and for zero noise are shown in Fig. 3(b). Note that exponential scaling is again well represented by the numerical data, including the behavior predicted by the prefactor  $\epsilon^{\text{const}}$  over a four decade range of  $\epsilon$ , as shown by the constant vertical (logarithmic) displacements of the data sets for each decade change in  $\epsilon$ . Figure 3(c) shows the accuracy of the scaling for noise intensities comparable to and much smaller than  $\epsilon$ . We see that the noise has little effect on the accuracy of the scaling so long as  $\xi \ll \epsilon$ . Figure 3(d) shows

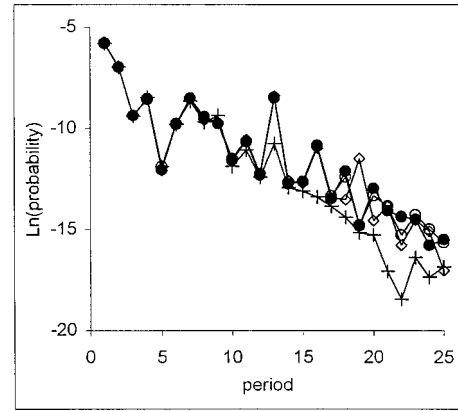


FIG. 4. Scaling of the encounter probability  $\Phi(p)$  versus period  $p$ , of UPOs in the Hénon map for  $a=1.4$  and  $b=0.3$  using the CR method. The symbols represent different noise intensities:  $\xi=0$  (solid circles),  $0.01\epsilon$  (open circles),  $0.1\epsilon$  (diamonds), and  $1.0\epsilon$  (plus signs) where  $\epsilon=0.01$ . Least-squares fits of Eq. (1) to these results give:  $Q=0.325$ ,  $0.326$ ,  $0.341$ , and  $0.443$  for  $\xi=0$ ,  $0.1\epsilon$ ,  $0.5\epsilon$ , and  $1.0\epsilon$ , respectively.

results again for four decades of  $\epsilon$  but with the noise held constant at  $\xi=0.01$ . These results show that, while exponential scaling remains the representative behavior, the value of the exponent  $Q$ , increases rapidly when  $\xi \gg \epsilon$ .

### B. The Hénon map

The Hénon map is given by

$$(x, y)_{n+1} \rightarrow (a - x_n^2 + b y_n + \xi_n, x_n + \xi'_n), \quad (14)$$

where the noises  $\xi_n$ , and  $\xi'_n$  are independent and were added to both iterates  $x$ ,  $y$ . Here we use the parameters  $a=1.4$  and  $b=0.3$ . The results of the CR method for  $\xi=0$  always, but for  $\xi'=0$ ,  $0.5\epsilon$ , and  $1.0\epsilon$ , where  $\epsilon=0.01$ , are shown in Fig. 4. We have matched the results to Eq. (1) using only the points  $p > 8$  with the result that  $Q=0.32 \pm 0.02$  for all noise values except the largest, for which  $\xi=\epsilon$ . The fit is performed only for the higher periods, because, first, the theory is accurate only for large  $p$ , and second, the Hénon map does not contain UPOs of periods  $p=3$  and  $5$ , though the CR method (and indeed any approximate search algorithm) will return some finite value for  $\Phi(p=3,5)$ . Thus the low period values of  $\Phi$  are not expected to exactly follow the scaling relation. As a check, we have also numerically calculated the first 32 periods by a different procedure<sup>41,42</sup> for zero and several different noise intensities again for  $\epsilon=0.01$ . In this case two noises,  $\xi$  and  $\xi'$ , were added to both  $x$  and  $y$  as shown by Eq. (14). These results are shown in Fig. 5(a) for zero noise and Fig. 5(b) for noise in the range  $10^{-3}\epsilon$  to  $1.0\epsilon$ . The values of  $Q$  are detailed in the caption of Fig. 5. Essentially,  $Q=0.41$  returns an underestimate of the known largest Lyapunov exponent for all noise values significantly smaller than  $\epsilon$ . As a comparative illustration, we have tested the DT method on short, 3000 point data files of the noise free Hénon map, as shown by the inset in Fig. 5(a). We see that the method, compared to results for suitable surrogates, is capable of detecting only periods 1 and 2. There is no period 3 in this map (but the method detects a small value), and

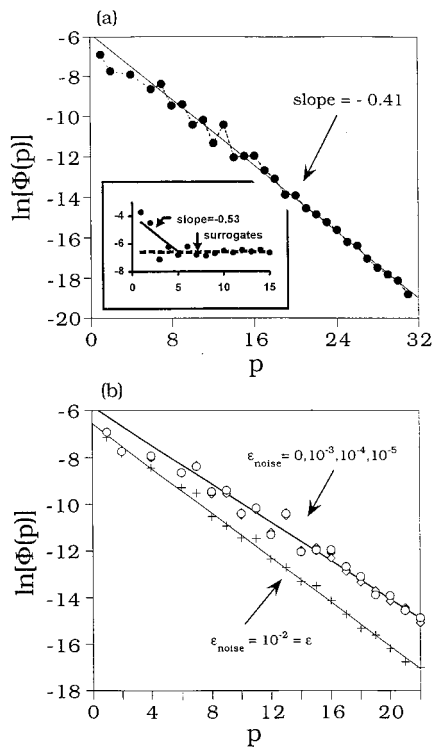


FIG. 5. Scaling of the encounter probability  $\Phi(p)$  versus period  $p$ , of UPOs in the Hénon map for  $a=1.4$  and  $b=0.3$  using the analytic method of Refs. 41 and 42 for  $\epsilon=0.01$ . (a) For zero noise, the straight line is a fit to Eq. (1) which gives  $Q=0.41$ . The inset shows the TR method applied to short data sets of this map for the same conditions. The straight line gives the estimate  $Q=0.53$ . The dashed line gives the mean background probability established by surrogate data sets. (b) The symbols show the scalings for different noise intensities:  $\xi=0$  (solid circles);  $0.001\epsilon$  (open circles),  $0.01\epsilon$  (shaded diamonds),  $0.1\epsilon$  (open diamonds), and  $1.0\epsilon$  (crosses). Least-squares fits of Eq. (1) (solid lines) give:  $Q=0.41$  for zero and all noises up to and including  $0.1\epsilon$  and  $0.48$  (14% larger) for the largest noise  $\xi=1.0\epsilon$ .

period 4 is at the level of the surrogates. See Ref. 26 for discussions of the use of this method and the generation and use of surrogate data sets.

### C. The Lorenz system

Because the TR and DT methods are finding their main applications to natural systems of unknown dynamics, it seems useful to test the proposed scaling relation on a widely known and used nonhyperbolic, or generic, system. The standard Lorenz system is given by

$$\begin{aligned}\dot{x} &= -10(x-y), \\ \dot{y} &= -y + 28x - xz, \\ \dot{z} &= -\beta z + xy + \xi_n,\end{aligned}\quad (15)$$

where  $\beta=8/3$ . These equations were integrated using the Runge-Kutta method with time step 0.01. The noise  $\xi_n$ , was chosen from a uniform distribution  $[-\xi, \xi]$  and updated at every time step  $n$ . The numerical data  $z(t)$ , were sampled at a sequence of times such that the time interval between samples was ten times larger than the time step used in the numerical integration. The times at which the samples were obtained were designated by an index  $n=1,2,\dots,N$ . Data sets

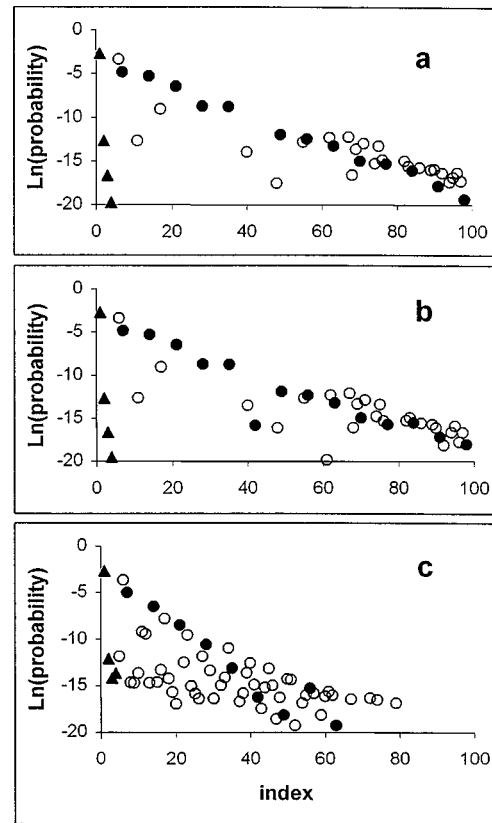


FIG. 6. Scaling of the encounter probability  $\Phi(p)$  versus period  $p$ , of UPOs in the standard Lorenz system for  $\beta=8/3$ . In all cases the file lengths were  $1.5 \times 10^9$ , and the neighborhood parameter was 1.0. The noise was taken from a uniform distribution  $[-\xi, \xi]$ . (a)  $\xi=0$ , (b)  $\xi=0.001$ , (c)  $\xi=0.1 \equiv 0.1\epsilon$ . In all cases the solid symbols show identified periods for  $q=1$  (solid triangles) and  $q=7$  (solid circles). The open circles represent complex behavior. Fits of the solid circles to the scaling relation give  $Q=0.157$ ,  $0.148$ , and  $0.253$  for  $\xi=0$ ,  $0.001$ , and  $0.1$ , respectively. These results show the exponential scaling behavior, but we cannot identify the points with specific periods.

of length  $N=10^8$  were generated and tested with the modified CR method. The encounter probabilities were obtained in the same way as for the maps and are shown in Fig. 6 but plotted against the index  $n$ . Periodic behavior can be identified by looking for sets of local maxima of  $\Phi(p)$  located at indices which are separated by a constant index distance  $q$ . Figure 6(a) shows the noise free results. We have identified two sets of periodic sequences:  $q=1$  (solid triangles) and  $q=7$  (solid circles). We cannot identify the specific periods within these two sets. For example, we might identify the 4th solid circle from the left as representing the encounter probability of the  $p=4$  orbit, but due to the ambiguity of the aforementioned set definition, the actual period of this orbit may be an integer multiple of 4. Nevertheless, the exponential scaling of the encounter probabilities with period is evident from the approximately linear behavior of the data on this plot.

### IV. SUMMARY AND DISCUSSION

Recent experimental work, primarily on biological systems, suggests that the probability to observe the signatures of unstable periodic orbits decreases exponentially with pe-

riod. In this work we have developed an approximate scaling theory of the encounter probability by associating it with estimates of the length of time a trajectory can shadow a periodic reference orbit within a small neighborhood. The theory indicates that the probability does indeed decrease exponentially with period, at least for large periods, and that the scaling parameter is related to the largest Lyapunov exponent and the entropies of the attractor. We have studied numerically the effects of noise and neighborhood size on this scaling in the logistic and Hénon maps and the standard Lorenz system using a modified CR method and, in the case of the Hénon map, a direct numerical method. In all tests, we find exponential scaling with the period regardless of the noise intensity, so long as that intensity is smaller than the neighborhood parameter.

We turn now to a brief discussion of the applicability of the theory and numerical simulations to the TR method. Why is this method uniquely successful at finding low period UPOs in short noisy data sets, and why can it not see high periods? The TR method detects the signatures of encounters with UPOs by searching for intersections of the unstable and stable manifolds (in two dimensions). It does so by examining returns to a Poincaré section and computing the perpendicular distances of the return points to the line of periodic points,  $x_{n+p} \equiv x_n$ . There must be a sequence of points with decreasing distances followed by a sequence with increasing distances, or  $m$  points in total ( $m$  is typically 5, see Refs. 20–23 and 26). The occurrence of these two connected sequences is the signature of a trajectory approaching the unstable periodic point at the intersection of the manifolds and then departing from it. If the definition of an encounter requires  $m$  total returns in the two sequences, then some degree of coherence must be maintained over a length  $mp$ . For high periods, this is a large number, which means that the probability to find a valid encounter becomes small. In practice, this probability drops to the level of the probability for chance findings as determined by the surrogates for periods of about four or greater. Thus the TR method fails to detect high period orbits. However, the signature of an encounter is a very specific sequence of points. See Refs. 20, 21, and 26 for details. By contrast the theory and the numerical methods, particularly the CR method, used here to find the encounter probabilities, require only that  $p$  returns fall within some neighborhood of size  $\epsilon$  of the periodic point. Thus significant coherence must be maintained only over a length  $p$  (instead of  $mp$  as required for the TR method). Moreover, the TR method successfully detects low period orbits in very noisy data sets because there is no small neighborhood condition. By contrast, as shown here, the CR method begins to fail when the noise intensity becomes comparable to the neighborhood size which, for accurate detection of high period orbits, must be small. These conditions evidently allow the TR method to detect low periods in short data sets while failing for higher periods. The CR method, in comparison, fails with short data sets, but can detect higher periods if very long data sets ( $10^8$ ) are available for which the noise intensity is smaller than the neighborhood size. The task to construct a theory of the encounter probability under the restrictive definitions used by the TR method for generic cha-

otic systems might be formidable, though an approximate calculation of this quantity for random files has been accomplished.<sup>54</sup>

Biological data, specifically recordings of the discharges from stimulated or unstimulated neurons, arise from the nonlinear dynamics of the neuron and its internal dynamical noise. Thus in seeking evidence of low dimensional dynamical behavior in biological preparations, one must have a method that can look down through the noise. Moreover, because biological preparations can at best be only approximately stationary, whatever analysis technique is adopted must be able to effectively deal with relatively short data sets. Finally, the state of stability of the dynamics is of prime interest in biology, because it is more likely to be successfully related to animal behavior. Thus the technique should also be able to distinguish stable from unstable periodic orbits and detect bifurcations between these behaviors. As we have shown here the TR method is well suited for these tasks. Moreover, it is numerically relatively simple, thus it is easy to implement and runs rapidly enough to be used on line during experiments. The latter feature is essential to applications involving control of chaos.<sup>55,56</sup>

The example biological data presented in Fig. 1 shows considerable scatter. These files were selected only on the basis that they show a significant number of period-2 orbits. They were thus obtained under various experimental conditions. The analogous situation in a physical system would be to collect orbits at random while varying the system parameters, then selecting all data sets showing any evidence of a period-2 orbit. Under these conditions large variability is to be expected. We show here the data selected in this way because it is probably typical of what might be expected of most biological systems where experimental conditions (parameters) cannot be nearly so well controlled as for physical systems. Our intention was to test the method and look for evidence of scaling using data as it might typically (rather than ideally) be encountered in biological preparations. Given the large variability typical of our biological data, it is problematic that we have successfully achieved our goal of connecting the three or four observable UPOs (see, for example, Fig. 1) with the infinite set. We have, however, provided a convincing reason for the rapid decrease in the observed encounter probabilities with period.

## ACKNOWLEDGMENTS

X.P. is supported by the Department of Energy, Electric and Magnetic Fields Program, X.P. and F.M. are supported by the Office of Naval Research, Physics Division. Y.C.L. is supported by the NSF under Grants No. PHY-9722156 and No. DMS-962659, and by the University of Kansas.

<sup>1</sup>*Measures of Complexity and Chaos*, edited by N. B. Abraham, A. M. Albano, A. Passamante, and P. Rapp (Plenum, New York, 1989).

<sup>2</sup>*Nonlinear Dynamics and Time Series: Building a Bridge between the Natural and Statistical Sciences*, edited by C. D. Cutler and D. T. Kaplan, Fields Institute Communications, Vol. 11 (American Mathematical Society, Providence, RI, 1996).

<sup>3</sup>See, for example, A. Wolf, J. B. Swift, H. L. Swinney, and J. A. Vastano, *Physica D* **16**, 285 (1985).

- <sup>4</sup>H. D. I. Abarbanel, R. Brown, J. J. Sidorowich, and L. S. Tsimring, *Rev. Mod. Phys.* **65**, 1331 (1993).
- <sup>5</sup>H. D. I. Abarbanel, *Analysis of Observed Chaotic Data* (Springer, New York, 1996).
- <sup>6</sup>See, for example, P. Grassberger and I. Procaccia, *Phys. Rev. Lett.* **50**, 346 (1983).
- <sup>7</sup>P. Grassberger and I. Procaccia, *Physica D* **13**, 34 (1984).
- <sup>8</sup>A. M. Albano, J. Muench, C. Schwartz, A. I. Mees, and P. E. Rapp, *Phys. Rev. A* **38**, 3017 (1988).
- <sup>9</sup>M. Ding, C. Grebogi, E. Ott, T. Sauer, and J. A. Yorke, *Phys. Rev. Lett.* **70**, 3872 (1993); *Physica D* **69**, 404 (1993).
- <sup>10</sup>P. E. Rapp, A. M. Albano, T. I. Schmah, and L. A. Farwell, *Phys. Rev. E* **47**, 2289 (1993).
- <sup>11</sup>Y.-C. Lai, D. Lerner, and R. Hayden, *Phys. Lett. A* **218**, 30 (1996).
- <sup>12</sup>K. A. Richardson, T. T. Imhoff, P. Grigg, and J. J. Collins, *Phys. Rev. Lett.* **80**, 2485 (1998).
- <sup>13</sup>D. Kaplan, *Physica D* **73**, 38 (1994); (personal communication); *Montreal 97 Summer School Lecture Notes, Week 2*, edited by The Faculty and Staff of the Centre for Nonlinear Dynamics (McGill University, Montreal, 1997), pp. 149–150.
- <sup>14</sup>G. Sugihara and R. M. May, *Nature (London)* **344**, 734 (1990).
- <sup>15</sup>M. Barahona and C.-S. Poon, *Nature (London)* **381**, 215 (1996).
- <sup>16</sup>D. P. Lathrop and E. J. Kostelich, *Phys. Rev. A* **40**, 4028 (1989).
- <sup>17</sup>G. Mindlin and R. Gilmore, *Physica D* **58**, 229 (1992).
- <sup>18</sup>G. Mindlin, H. Solari, M. Natiello, R. Gilmore, and X.-J. Hou, *Nonlinear Science* **1**, 147 (1991).
- <sup>19</sup>R. Gilmore, R. Vilaseca, R. Corbalan, and E. Roldan, *Phys. Rev. E* **55**, 2479 (1997).
- <sup>20</sup>D. Pierson and F. Moss, *Phys. Rev. Lett.* **75**, 2124 (1995).
- <sup>21</sup>X. Pei and F. Moss, *Nature (London)* **379**, 618 (1996).
- <sup>22</sup>X. Pei and F. Moss, *Int. J. Neural Syst.* **7**, 429 (1996).
- <sup>23</sup>H. A. Braun, K. Schäfer, K. Voigt, R. Peters, F. Bretschneider, X. Pei, L. Wilkens, and F. Moss, *J. Comp. Neurosci.* **4**, 335 (1997).
- <sup>24</sup>P. So, E. Ott, S. Schiff, D. T. Kaplan, T. Sauer, and C. Grebogi, *Phys. Rev. Lett.* **76**, 4705 (1996).
- <sup>25</sup>P. So, E. Ott, T. Sauer, B. J. Gluckman, C. Grebogi, and S. Schiff, *Phys. Rev. E* **55**, 5398 (1997).
- <sup>26</sup>M. Spano, X. Pei, K. Dolan and F. Moss (to be published).
- <sup>27</sup>D. Auerbach, P. Cvitanovic, J.-P. Eckmann, G. H. Gunaratne, and I. Procaccia, *Phys. Rev. Lett.* **58**, 2387 (1988).
- <sup>28</sup>P. Cvitanovic, *Phys. Rev. Lett.* **61**, 2729 (1988).
- <sup>29</sup>R. Artuso, E. Aurell, and P. Cvitanovic, *Nonlinearity* **3**, 325 (1990).
- <sup>30</sup>R. Artuso, E. Aurell, and P. Cvitanovic, *Nonlinearity* **3**, 361 (1990).
- <sup>31</sup>P. Cvitanovic, *Physica D* **51**, 138 (1991).
- <sup>32</sup>R. Badii, *Complexity-Hierarchical Structures and Scaling in Physics* (Cambridge University Press, Cambridge, England, 1997).
- <sup>33</sup>R. Badii, E. Brun, M. Finardi, L. Flepp, R. Holzner, J. Parisi, C. Reyl, and J. Simonet, *Rev. Mod. Phys.* **66**, 1389 (1994).
- <sup>34</sup>T. C. Halsey, M. H. Jensen, L. P. Kadanoff, I. Procaccia, and B. Shraiman, *Phys. Rev. A* **33**, 1141 (1986).
- <sup>35</sup>P. Grassberger, R. Badii, and A. Politi, *J. Stat. Phys.* **51**, 135 (1988).
- <sup>36</sup>R. Badii, *Riv. Nuovo Cimento* **12**, 1 (1989).
- <sup>37</sup>C. Beck and F. Schlögel, *Thermodynamics of Chaotic Systems* (Cambridge University Press, Cambridge, England, 1993).
- <sup>38</sup>R. Badii, *Chaos* **7**, 694 (1997).
- <sup>39</sup>R. Badii, *Phys. Rev. E* **54**, R4496 (1996).
- <sup>40</sup>Effectively,  $\text{const} \approx \langle \alpha \rangle$ , since averaging over initial conditions is an approximate effect of dynamical noise in experimental systems.
- <sup>41</sup>O. Biham and W. Wenzel, *Phys. Rev. Lett.* **63**, 819 (1989).
- <sup>42</sup>O. Biham and W. Wenzel, *Phys. Rev. A* **42**, 4639 (1990).
- <sup>43</sup>Y.-C. Lai, X. Pei, and F. Moss (to be published).
- <sup>44</sup>K. T. Alligood, T. D. Sauer, and J. A. Yorke, *Chaos: An Introduction to Dynamical Systems* (Springer, New York, 1997).
- <sup>45</sup>A. Renyi, *Probability Theory* (North-Holland, Amsterdam, 1970).
- <sup>46</sup>J.-P. Eckmann and D. Ruelle, *Rev. Mod. Phys.* **57**, 617 (1985).
- <sup>47</sup>C. Grebogi, E. Ott, and J. A. Yorke, *Phys. Rev. A* **37**, 1711 (1988).
- <sup>48</sup>E. Ott, *Chaos in Dynamical Systems* (Cambridge University Press, New York, 1993).
- <sup>49</sup>Y.-C. Lai, Y. Nagai, and C. Grebogi, *Phys. Rev. Lett.* **79**, 649 (1997).
- <sup>50</sup>In general, it can be proven that the metric entropy is at most the sum of the positive Lyapunov exponents [e.g., D. Ruelle, *Chaotic Evolution and Strange Attractors* (Cambridge University Press, New York, 1989)]. For a low-dimensional chaotic system with one positive Lyapunov exponent  $\lambda$ , we thus have  $K_1 \leq \lambda$ . The topological entropy  $K_0$  and the metric entropy  $K_1$  are two members of the generalized entropies  $K_q$ , which satisfy  $K_0 \geq K_1$ . It is also known that for a two-dimensional smooth invertible map, the Kaplan-Yorke conjecture reduces to the equality  $K_1 = \lambda$  [J. L. Kaplan and J. A. Yorke, in *Functional Differential Equations and Approximations of Fixed Points*, edited by H.-O. Peitgen and H.-O. Walter, Lecture Notes in Mathematics Vol. 730 (Springer, Berlin, 1979)].
- <sup>51</sup>The dynamics is hyperbolic on a chaotic attractor if at each point of the trajectory the phase space can be split into an expanding and a contracting subspace, and the angle between them is bounded away from zero. Furthermore, the expanding subspace evolves into the expanding one along the trajectory and the same is true for the contracting subspace. Otherwise the set is nonhyperbolic (Ref. 39).
- <sup>52</sup>R. Bowen, *On Axiom A Diffeomorphisms*, CBMS Regional Conference Series in Mathematics (American Mathematical Society, Providence, RI, 1978), Vol. 35.
- <sup>53</sup>J. C. Sprott and G. Rowlands, *Chaos Data Analyzer* (American Institute of Physics, New York, 1995).
- <sup>54</sup>K. Dolan, *Bull. Am. Phys. Soc.* **42**, 815 (1997).
- <sup>55</sup>W. L. Ditto, S. N. Rauseo, and M. L. Spano, *Phys. Rev. Lett.* **65**, 3211 (1990).
- <sup>56</sup>A. Garfinkel, M. L. Spano, W. L. Ditto, and J. N. Weiss, *Science* **257**, 1230 (1992).